Development 130, 1267-1280

doi:10.1242/dev.00351

BDNF regulates spontaneous correlated activity at early developmental stages by increasing synaptogenesis and expression of the K^+/Cl^- co-transporter KCC2

Fernando Aguado[1,*], Maria A. Carmona[1,*], Esther Pozas[1], Agustín Aguiló[1], Francisco J. Martínez-Guijarro[2], Soledad Alcantara[1], Victor Borrell[1], Rafael Yuste[3], Carlos F. Ibañez[4] and Eduardo Soriano[1,†]

[1]Department of Cell Biology Faculty of Biology, and Barcelona Science Park, University of Barcelona, Barcelona 08028, Spain
[2]Department of Cell Biology, Faculty of Biological Sciences, University of Valencia, 46100 Burjassot, Spain
[3]Department of Biological Sciences, Columbia University, New York, New York 10027, USA
[4]Department of Neurosciences, Karolinska Institute, Stockholm 17177, Sweden
*These authors contributed equally to this study
[†]Author for correspondence (e-mail: soriano@porthos.bio.ub.es)

Accepted 18 December 2002

SUMMARY

Spontaneous neural activity is a basic property of the developing brain, which regulates key developmental processes, including migration, neural differentiation and formation and refinement of connections. The mechanisms regulating spontaneous activity are not known. By using transgenic embryos that overexpress BDNF under the control of the *nestin* promoter, we show here that BDNF controls the emergence and robustness of spontaneous activity in embryonic hippocampal slices. Further, BDNF dramatically increases spontaneous co-active network activity, which is believed to synchronize gene expression and synaptogenesis in vast numbers of neurons. In fact, BDNF raises the spontaneous activity of E18 hippocampal neurons to levels that are typical of postnatal slices.

We also show that BDNF overexpression increases the number of synapses at much earlier stages (E18) than those reported previously. Most of these synapses were GABAergic, and GABAergic interneurons showed hypertrophy and a 3-fold increase in GAD expression. Interestingly, whereas BDNF does not alter the expression of GABA and glutamate ionotropic receptors, it does raise the expression of the recently cloned K^+/Cl^- KCC2 co-transporter, which is responsible for the conversion of GABA responses from depolarizing to inhibitory, through the control of the Cl^- potential. Together, results indicate that both the presynaptic and postsynaptic machineries of GABAergic circuits may be essential targets of BDNF actions to control spontaneous activity. The data indicate that BDNF is a potent regulator of spontaneous activity and co-active networks, which is a new level of regulation of neurotrophins. Given that BDNF itself is regulated by neuronal activity, we suggest that BDNF acts as a homeostatic factor controlling the emergence, complexity and networking properties of spontaneous networks.

Key words: Synaptogenesis, KCC2, Spontaneous activity, CNS, BDNF, Mouse, GABA, Ca^{2+} oscillations

INTRODUCTION

Spontaneous neuronal activity is a common feature of the developing CNS, which is required for neurite extension, neuronal migration and differentiation, and for the formation and refinement of neural circuits (Katz and Shatz, 1996; Komuro and Rakic, 1998; Penn et al., 1998; Spitzer et al., 2000; Stellwagen and Shatz, 2002). An important feature of spontaneous activity is the occurrence of synchronous patterns of co-activation across tens to hundreds of neurons, which are believed to reflect the complexity of the intrinsic circuit (Yuste et al., 1992; Feller, 1999; O'Donovan, 1999). The emergence of spontaneous network activity is developmentally regulated and occurs when the excitation is high enough to sustain the regenerative recruitment of the whole network (Feller, 1999; O'Donovan, 1999). Correlated patterns of spontaneous activity may synchronize both neuronal activity and gene expression, thus amplifying the functional consequences of activity to control neuronal development (Buonanno and Fields, 1999; O'Donovan, 1999).

Although certain signaling mechanisms, particularly neurotransmitters and gap junctions, are thought to sustain spontaneous activity, the signals regulating the formation and complexity of spontaneous co-active networks have not been identified (Yuste et al., 1995; Ben-Ari et al., 1997; Garaschuk et al., 1998; Feller, 1999; O'Donovan, 1999; Ben-Ari, 2001). The neurotrophin family exerts potent trophic actions in the peripheral and central nervous systems (PNS and CNS) through the tyrosine kinase receptors TrkA, TrkB and TrkC, and the death domain-containing p75 receptor

(Huang and Reichardt, 2001). Neurotrophins are also associated with the structural and functional regulation of axonal and dendritic growth, synapse formation and synaptic transmission (Huang et al., 1999; McAllister et al., 1999; Schuman, 1999; Schinder and Poo, 2000; Alsina et al., 2001; Huang and Reichardt, 2001). In contrast, whether neurotrophins regulate the emergence and patterns of spontaneous neuronal activity at early developmental stages is currently unknown. We now show that, in vivo, overexpression of BDNF regulates the onset and complexity of spontaneous correlated network activity from very early stages of development. We also show that higher rates of synaptogenesis and GABA production, and the expression of the KCC2 co-transporter, which controls intracellular [Cl^-] level, underlie the effects of BDNF on coordinated network activity.

MATERIALS AND METHODS

Animals

Mice overexpressing BDNF were generated as described previously (Ringstedt et al., 1998). The *nestin*-BDNF construct was injected into fertilized mouse oocytes, which were transplanted into pseudopregnant females. The offspring (at E18) were screened for founders by PCR.

Histological techniques

DiI tracing

Small crystals of the lipophilic tracer DiI (Molecular Probes) were placed in the entorhinal cortex of paraformaldehyde-fixed wild-type (n=4) and transgenic (n=3) brains and horizontal sections were counterstained with bisbenzimide (Sigma) (Barallobre et al., 2000).

Immunocytochemistry

Free-floating sections (Barallobre et al., 2000) from four wild-type and four transgenic brains were incubated with the following primary antibodies: GluR1, GluR2/3 and synapsin I (Chemicon), synaptophysin and syntaxin 1 (Sigma), NMDAR1 and NMDAR2A (Watanabe et al., 1998), $GABA_A$ α1 and $GABA_A$ α2 (Fritschy et al., 1994), calbindin and calretinin (Swant, Bellizona, Switzerland). Sections were processed using the Vectastain ABC kit (Vector Laboratories, UK).

In situ hybridization

Non-radioactive hybridizations were performed on three transgenic and four control brains according to the method of Barallobre et al. (Barallobre et al., 2000). RNA probes against the two rat glutamic decarboxylase isoforms (GAD_{65} and GAD_{67}) have been described previously (Erlander et al., 1991). To obtain the KCC2 riboprobe, RNA from mouse brain was reverse-transcribed with M-MuLV (Biolabs), and a 474 pb fragment of mouse KCC2 (AF332064 GenBank database) was amplified by PCR (forward primer: 5′-CTCAACAACCTGACGGACTG-3′; reverse primer: 5′-GCACAACACCATTGGTT GCG-3′).

Electron microscopy

Four wild-type and five transgenic brains were prepared for EM analysis (Crespo et al., 2000) and electron micrographs were randomly taken from the stratum radiatum of the CA1 region at a final magnification of ×26,000. Vesicles were considered docked when their membrane was less than 50 nm from the presynaptic active zone (Rosahl et al., 1995). Post-embedding GABA immunostaining followed the method described by Crespo et al. (Crespo et al., 2000), using a rabbit anti-GABA antiserum and 10 nm colloidal gold-coated secondary antibodies (Sigma). Electron micrographs at final magnifications of ×52,000 were taken at random from the stratum radiatum.

Biochemical and molecular techniques

Western blotting

The proteins of total membrane fractions from the forebrains of 3 transgenic BDNF-overexpressing mice and 3 control littermates were separated by 8% and 10% SDS-PAGE and electrotransferred to a nitrocellulose membrane. The membranes were incubated with the same primary antibodies used for immunocytochemical assays, and with an anti-ATPase β1 (Upstate Biotechnology) and bound Igs were viewed using the ECL chemiluminescent system (Amersham). Densitometric analysis, standardized to ATPase β1, was performed using Imat software.

Northern blotting

Twenty μg of total RNA from two BDNF transgenic and two control forebrains per sample were hybridized with BDNF (484-825 bp in the coding sequence of mouse BDNF) and GAD_{67} (Erlander et al., 1991) cDNA probes labeled with ^{32}P. The same filters were rehybridized with a mouse cyclophilin cDNA probe to standardize RNA. Autoradiograms were quantified as above.

Reverse transcription-PCR and southern hybridization

One μg of total RNA from each forebrain was retrotranscribed and amplified using the Reverse Transcription System (Promega). Amplification was run up to 25 cycles with *taq* polymerase. For the KCC2 assays the forward and reverse primers described above were utilized. For glyceraldehyde phosphate dehydrogenase (GAPDH) assays the forward primer was GGCCCCTCTGGAAAGCTGTGG, and the reverse primer was CCTTGGAGGCCATGTAGGCCAT (608 to 1043 nucleotides of mouse GADPH). Autoradiograms of Southern blots of PCR products were quantified as above.

Imaging

Neuronal activity was recorded on hippocampal acute slices (E16-P5 stages) (Schwartz et al., 1998; Aguiló et al., 1999). The brains were removed into ice-cold artificial cerebrospinal fluid (ACSF) solution composed of (in mM): NaCl 120, KCl 3, D-glucose 10, $NaHCO_3$ 26, NaH_2PO_4 2.25, $CaCl_2$ 2, $MgSO_4$ 1, pH 7.4, bubbled with 95% O_2 and 5% CO_2. Transverse hippocampal slices (300 μm) were incubated with the Ca^{2+} indicator fura-2-AM (Molecular Probes, Eugene, OR). Images were captured in an upright fluorescence microscope (BX50WI; Olympus, Tokyo, Japan) at room temperature (22-25°C) with a silicon-intensifier tube (SIT) camera (Hamamatsu C2400-08). Fura-2 fluorescence images were collected at 4 second intervals (15 frames average for each time point) using a 380 nm bandpass filter controlled by the NIH Image program. (±)-2-amino-5-phosphonopentanoic acid (APV), 6-cyano-7-nitroquinoxaline-2, 3-dione (CNQX) and (–)-bicuculline methiodide (BMI) were obtained from Sigma.

Network analysis

Changes in fluorescence, $\Delta F/F=(F_0-F_1)/(F_0)$, were analyzed with a program written in Interactive Data Language (IDL; Research Systems Inc., Boulder, CO) (Schwartz et al., 1998; Aguiló et al., 1999). The time of initiation of each Ca^{2+} transient for each cell was marked in a raster plot. These raster plots were used to calculate the matrix of asymmetric correlation coefficients between all cell pairs. Contingency tables and χ^2 tests were then used to detect which of the correlation coefficients was significantly greater than expected. Significant correlation coefficients were used to generate a correlation map in which lines link neurons whose asymmetric correlation coefficient is significant ($P<0.01$) and in which the thickness of a line connecting any two cells represents the magnitude of the greatest

asymmetric correlation coefficient between the cells (Schwartz et al., 1998; Aguiló et al., 1999).

To test whether the $[Ca^{2+}]_i$ transients showed associations between the neurons within a network, the number of simultaneous activations in a recording was measured and used as a statistical test (Schwartz et al., 1998; Aguiló et al., 1999). To determine its *P* value, the distribution of the statistics under the null hypothesis of independent transients was computed by Monte Carlo simulation. The *P* value was then estimated as the proportion of the 1,000 replications in which the statistical test exceeded the statistical test computed from the real data. To simulate independent realizations of the transients, the number of cells, activations and time intervals were preserved, but the initiations of the transients were taken at random.

Statistics

The Student's *t*, Mann-Whitney U and Bernouilli tests were used. Data are expressed as mean ± s.e.m.

RESULTS

Spontaneous synchronous network activity emerges at late embryonic stages in the hippocampus

Spontaneous network activity occurs in the postnatal hippocampus (Ben-Ari et al., 1997; Garaschuk et al., 1998; Ben-Ari, 2001). However, hippocampal afferents develop before birth (Supèr and Soriano, 1994) and excitatory postsynaptic potentials have been recorded in the prenatal hippocampus (Diabira et al., 1999). We therefore examined the emergence of spontaneous network activity at early stages of development using calcium imaging. After fura-2-AM incubation of hippocampal slices, most dye-loaded cells were located in the principal neuronal layers, corresponding to pyramidal and granule cells. Some fluorescent cells, with the appearance of interneurons, were also seen in the plexiform layers (Fig. 1A). We monitored spontaneous changes in $[Ca^{2+}]_i$ for 10-20 minutes simultaneously in many neurons of the field (Fig. 2A,F) (see Schwartz et al., 1998; Aguiló et al., 1999). No spontaneous activity was recorded before embryonic day 15 (E15). From E16 onwards, spontaneous $[Ca^{2+}]_i$ transients were observed in all the subfields of the hippocampus. Spontaneous changes in $[Ca^{2+}]_i$ were rare at embryonic stages, but very frequent at postnatal stages. Most $[Ca^{2+}]_i$ oscillations lasted from 8 to 60 seconds, and their amplitude and decay time were variable (Fig. 1B,C).

We focused on the CA1 region and measured both the number of active cells and the frequency of Ca^{2+} oscillations. Few active cells were recorded at E16-E17 (Fig. 1D), but the number increased at E18 and around birth (postnatal days 0-1, P0-P1). There was a 2- to 3-fold increase in the number of active neurons at P2-P5 over P0. Similarly, the rate of activation per neuron increased from prenatal to postnatal stages, with a maximum between P2 and P5 (Fig. 1E). We conclude that spontaneous neuronal activity in the hippocampus emerges at E16 and reaches highest levels during postnatal development.

We represented the profile of activation of every active cell in each movie in raster plots (Fig. 2A-C,F,G). By comparing the raster plots of embryonic and postnatal stages, we observed that the number of apparent synchronous firing events increased with age (Fig. 2C,G). We next used a statistical analysis based on contingency tables and χ^2 tests to identify pairs of cells with significant synchronous activity (Schwartz et al., 1998; Aguiló et al., 1999). This analysis results in correlation maps illustrating networks of co-active cells, in which each pair of synchronous cells is connected by lines

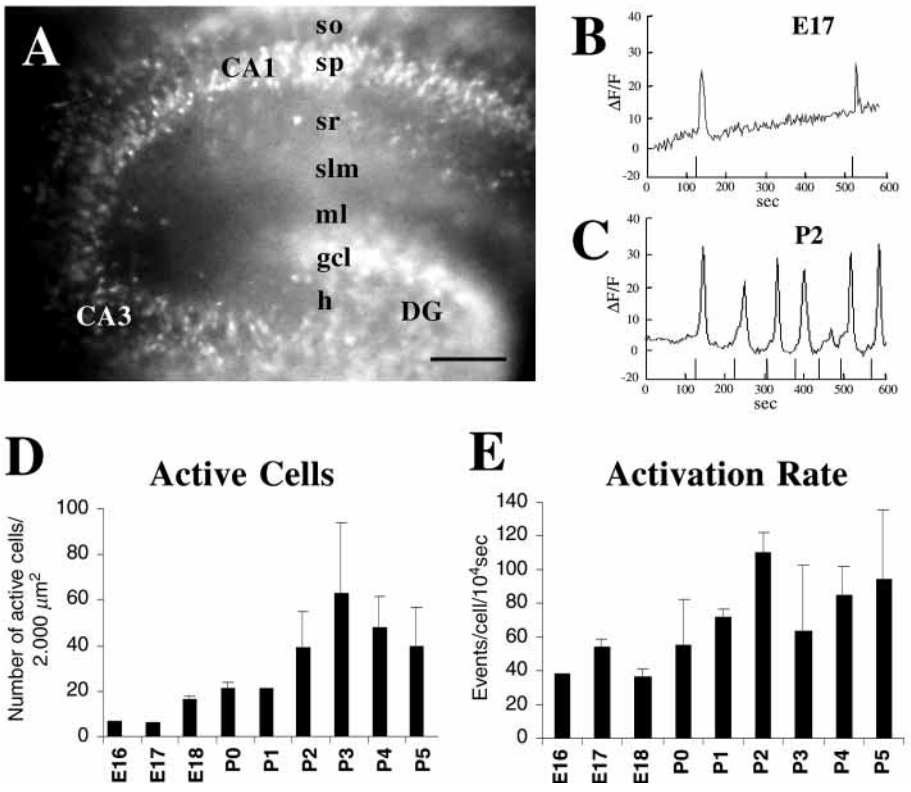

Fig. 1. Developmental regulation of spontaneous $[Ca^{2+}]_i$ oscillations in the embryonic and postnatal hippocampus. (A) Horizontal hippocampal slice from an E18 embryo loaded with fura-2-AM. The principal cells (pyramidal and granular neurons) and some interneurons show intense fura-2 fluorescence. Scale bar: 400 μm. (B,C) Representative plots of ΔF/F over time showing spontaneous $[Ca^{2+}]_i$ transients in CA1 hippocampal neurons at E17 (B) and P2 (C). The onset of each $[Ca^{2+}]_i$ oscillation is indicated by a bar on the x axis. Note the greater number of spontaneous Ca^{2+} events at postnatal ages than at embryonic ages. (D,E) Histograms illustrating the developmental regulation of the number of spontaneously active cells/2,000 μm^2 (D) and their activation rate ($[Ca^{2+}]_i$ oscillations/cell/10^4 seconds) (E) from E16 to P5. Both parameters increase around birth and peak at P2-P5. Values are shown as mean ± s.e.m. CA1 and CA3, hippocampal regions; DG, dentate gyrus; h, hilus; gcl, granule cell layer; ml, molecular layer; slm, stratum lacunosum moleculare; so, stratum oriens; sp, stratum piramidale; sr, stratum radiatum.

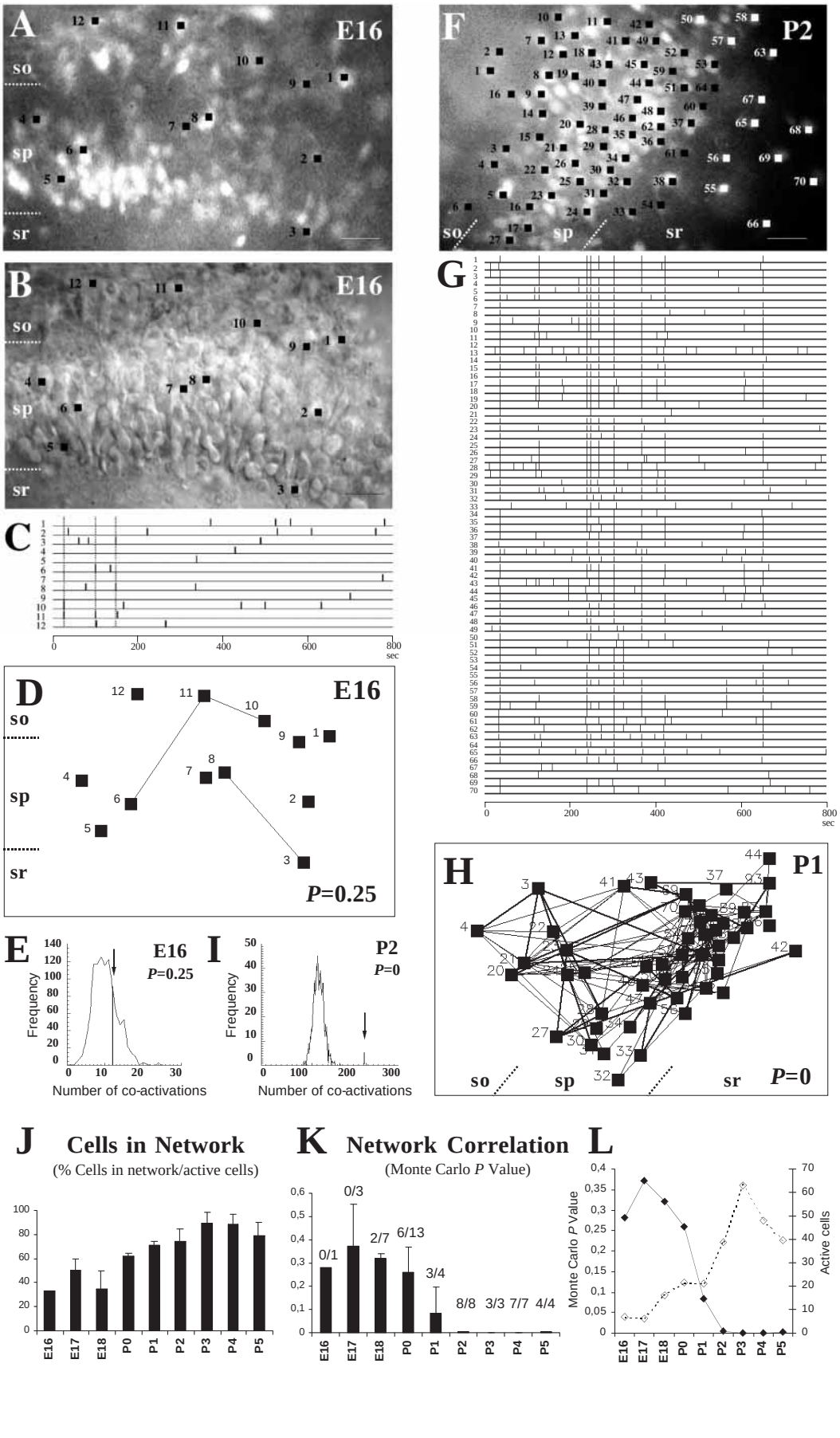
A
E16
so
sp
sr
B
E16
so
sp
sr
C
0
200
400
600
800
sec
D
E16
so
sp
sr
P=0.25
E
E16
P=0.25
Frequency
Number of co-activations
I
P2
P=0
Frequency
Number of co-activations
F
P2
so
sp
sr
G
0
200
400
600
800
sec
H
P1
so
sp
sr
P=0
J
Cells in Network
(% Cells in network/active cells)
E16
E17
E18
P0
P1
P2
P3
P4
P5
K
Network Correlation
(Monte Carlo P Value)
0/1
0/3
2/7
6/13
3/4
8/8
3/3
7/7
4/4
E16
E17
E18
P0
P1
P2
P3
P4
P5
L
Monte Carlo P Value
Active cells
E16
E17
E18
P0
P1
P2
P3
P4
P5

Fig. 2. Synchronous patterns of spontaneous network activity in the hippocampal CA1 region emerge after birth. (A-E) Correlation network analysis of the CA1 hippocampal region at E16. (A,B) Paired photomicrographs showing the same field viewed under fura-2 fluorescence (A) and DIC optics (B) illustrating dozens of cells loaded with the Ca^{2+} indicator. Black squares indicate cells with spontaneous changes of fura-2 fluorescence signal over time. (C) Raster plot representing the activity profile of each of the 12 spontaneously active cells shown in A and B over 800 seconds. The activity profiles of individual cells are represented by horizontal lines and each tick mark labels the onset of each Ca^{2+} transient. Dotted lines indicate simultaneous onset of $[Ca^{2+}]_i$ oscillations of at least two cells of the plot. Note the small number of co-activations at E16 (e.g. cells no. 6 and no. 11). (D) Spatiotemporal correlation map illustrating all the active cells shown in A-C, in which pairs of cells with statistically significant correlation coefficients are linked by lines. Only 5 out of 12 active cells, located in the stratum oriens and in the pyramidal layer, show significant synchrony. The *P* value reflects the probability that the overall degree of synchronous correlation present in this network is caused by chance (see E). (E) Distribution of pair-wise correlations found in the real data (arrow) and in 1,000 simulations obtained by the Monte Carlo test (bell-shaped curve) of the active cells shown in A-D (see Materials and Methods). In this case, the number of correlated events in the real data set (arrow) does not exceed that expected by chance in simulated data, $P=0.25$. (F-I) Correlation network analysis of the CA1 hippocampal region at P1-P2. (F) CA1 region of a P2 hippocampal slice viewed with fura-2 fluorescence. Note the greater number of active cells (squares) than at E16 (A). (G) Raster plot illustrating the activity profile of each of the 70 cells shown in F. Highly synchronous activity patterns, in which network oscillations involve virtually the entire population of active neurons, are easily recognized. (H) Spatiotemporal correlation map of the CA1 region of a P1 slice illustrating complex synchronous networks, which recruit vast populations of active cells. Note the greater overall complexity than at E16. Furthermore, the lines connecting co-active cells are thicker than at E16, indicating higher degrees of correlation. The *P* value reflecting the probability that the overall degree of synchronous correlation present in this network is caused by chance is 0 (see I). (I) The number of simultaneous co-activations present in the network represented in H (arrow) exceeds the frequency distribution of random experiments created by Monte Carlo simulation. (J) Percentages of active cells involved in synchronous correlated networks at different ages (E16-P5). (K) Average of *P* values representing network correlation during development. The number of cases with significant synchronous correlated networks ($P<0.05$) in relation to the total number of cases analyzed is shown at the top of each bar. (L) Graph illustrating the correlation between the rise in network synchrony (*P* values, left, solid line) and the increase in the number of active cells (dotted line; see Fig. 1D) in the hippocampal CA1 region during development. Values in J and K are given as mean ± s.e.m. Scale bars, 40 μm. Abbreviations as in Fig. 1.

whose thickness is proportional to the degree of correlation (see Materials and Methods) (Fig. 2D,H). Very simple correlation maps were observed at E16-E17 (Fig. 2D), whereas the complexity of the networks increased at E18-P1 (Fig. 2H). From P2 onwards, virtually every active neuron displayed synchronous firing, resulting in complex correlation maps in which all active neurons were recruited into synchronous Ca^{2+} waves (not shown, see raster plot in Fig. 2G). The percentage of active cells with correlated activity increased progressively from 33% at E16 to 78-94% at P3-P5 (Fig. 2J), demonstrating that most active cells formed part of a coordinated network at early postnatal stages.

We also measured the overall degree of synchronous correlation in each network sample, by comparing the number of times any two cells showed simultaneous onset of activation in the actual experiment (number of co-activations) with the number of co-activation events present in a theoretical distribution of 1,000 data sets created by random Monte Carlo simulation (Schwartz et al., 1998). This comparison gives a *P* value for the experimental data set that describes the probability that the entire number of co-activations present in each sample was random (Fig. 2E,I). Because the simulations are performed with the same number of neurons as in the actual experiment, the statistical significance of the correlation is independent of the number of neurons forming part of a given network (Schwartz et al., 1998; Aguiló et al., 1999). The first significant overall correlated networks ($P<0.05$) were found at E18 (2 out of 7), and more were found at P0-P1 (9 out of 17). In contrast, all 22 samples recorded at P2-P5 showed significant correlations, indicating the generation of highly synchronous networks (Fig. 2K). The developmental rise of synchronous networks (statistically significant *P* values) parallels a non-linear increase in the number of active cells (Fig. 2L), suggesting that a threshold of active neurons is required to generate complex patterns of synchronous activity.

These results show that spontaneous activity in the hippocampus increases progressively from embryonic to postnatal stages, with significant synchronized network activity emerging only after E18. However, not until P2 does spontaneous neuronal activity became organized into highly complex patterns of synchronous activity.

BDNF overexpression enhances spontaneous correlated network activity at embryonic stages

We examined the role of BDNF in the regulation of spontaneous correlated networks at early stages in vivo, in transgenic mice overexpressing BDNF under the control of the *nestin* promoter, which drives transgene expression to CNS progenitors from E10, a few days before the onset of endogenous BDNF production (Ringstedt et al., 1998). Expression of the specific BDNF receptor TrkB in the forebrain begins at E13 (Knüsel et al., 1994). As these transgenic mice die of cardiac malfunction soon after birth (Ringstedt et al., 1998), embryos were analyzed at E18. Littermate embryos, with no integration of the transgene, were used as controls.

At E18, BDNF mRNA was barely detectable in control embryonic forebrains, whereas *nestin*-BDNF transgenic forebrains showed conspicuous BDNF mRNA expression, as determined by northern blot analysis (Fig. 3A). In contrast to the neocortex (Ringstedt et al., 1998), most *nestin*-BDNF transgenic mice displayed normal hippocampal cytoarchitectonics, with the pyramidal and granule neurons arranged in single layers. However, some of the embryos with the highest number of integrated transgenes showed a double-pyramidal layer in the CA3-CA1 region (Fig. 3B,C). The remaining neuronal populations of the embryonic hippocampus (Supèr et al., 1998), including Cajal-Retzius cells and GABAergic interneurons, appeared well-positioned, as shown by reelin (data not shown), calretinin, glutamic acid decarboxylase (GAD) and calbindin labelling (Fig. 3D,E, Fig. 7A,B,D,E). Immunostaining for the adhesion molecule L1 (Fig. 3F) and axonal tracing of the main hippocampal afferents by injections of the tracer DiI (Fig. 3G), showed that axonal

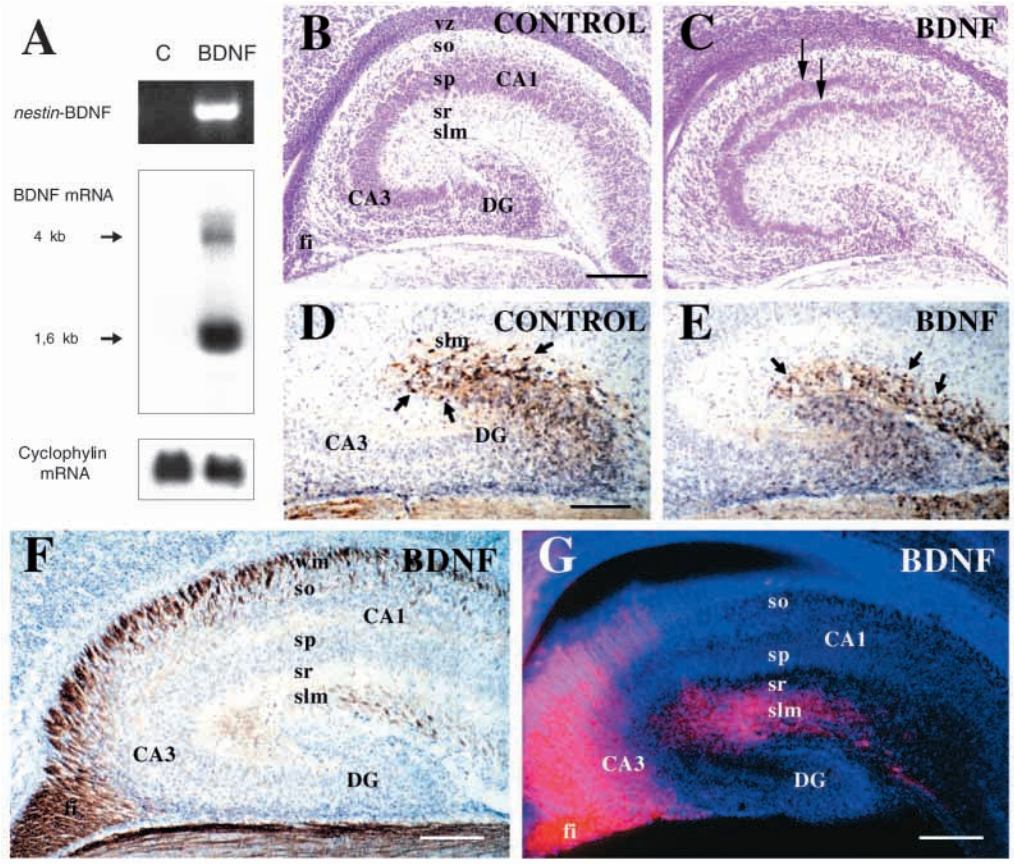

Fig. 3. Histological organization of the hippocampus in transgenic BDNF-overexpressing embryos. (A) Transgenic (BDNF) and control (C) E18 embryos are identified by PCR analysis of the *nestin*-BDNF construct. As revealed by northern blot analysis, *nestin*-BDNF transgenic forebrains express about 30-fold higher levels of BDNF mRNA than controls (including endogenous and transgenic mRNAs). Cyclophilin mRNA levels were used as an internal standard. (B,C) Nissl staining of BDNF-overexpressing and control hippocampal sections. The overall hippocampal cytoarchitectonics is preserved in transgenic hippocampi, although transgenic embryos that integrated many construct copies show a double pyramidal layer (arrows in C). (D,E) Calretinin immunostaining shows the correct location of Cajal-Retzius cells in the stratum lacunosum-moleculare (arrows) in both transgenic and wild-type hippocampi. (F) Section from the hippocampus of a BDNF transgenic embryo immunolabeled by the axonal marker L1, showing correct axonal patterns with L1-positive fascicles in the white matter (wm), fimbria (fi) and in the stratum lacunosum-moleculare (slm), mainly corresponding to commissural and entorhino-hippocampal axons. (G) Patterns of entorhino-hippocampal innervation in a BDNF transgenic hippocampus following a DiI injection in the entorhinal cortex. Entorhinal fibers (red) are seen in the fimbria (fi) and in the stratum lacunosum-moleculare (slm). Section counterstained with bisbenzimide (blue). Scale bars, 400 μm. Abbreviations as in Fig. 1.

Fig. 4. BDNF-overexpressing hippocampi show increased spontaneous correlated network activity at E18. (A-H) Representative examples of network activity in the hippocampal CA1 region in control (A-D) and transgenic (E-H) E18 embryos. (A) Fura-2-loaded control hippocampal slice showing few active neurons (squares). (B) Plot of ΔF/F over time illustrating spontaneous $[Ca^{2+}]_i$ changes in a control neuron. The initiation of $[Ca^{2+}]_i$ transients is indicated by bars on the x axis. (C) Raster plots of all active cells shown in A. Horizontal lines represent the activity profile over 800 seconds of each active neuron and vertical thick lines mark the onset of $[Ca^{2+}]_i$ oscillations. (D) Correlation map illustrating a significant ($P<0.01$) spatio-temporal co-activation among all cell pairs shown in A and C assayed with χ^2 contingency tables. The thickness of the lines is proportional to the degree of significance. The *P* value indicated at the bottom ($P=0.15$) reflects the overall level of co-activation obtained by Monte Carlo simulation, and represents the probability that the co-activations present in this field are caused by chance. (E) Fura-2-loaded transgenic hippocampal slice illustrating more active neurons (squares) than in controls. (F) Representative plot of ΔF/F over time showing spontaneous $[Ca^{2+}]_i$ oscillations in a hippocampal neuron from a transgenic embryo. (G) Raster plot of all active neurons shown in E, illustrating the activity profile of each of the 49 cells over 800 seconds. Note the greater number of active neurons, $[Ca^{2+}]_i$ transients and co-activations than in C. (H) Correlation map showing the spatio-temporal co-activations present in the transgenic CA1 region shown in E. BDNF-overexpression increases the complexity of spontaneous correlated networks in the hippocampus. Furthermore, the overall synchrony of this network also increases in BDNF transgenic embryos, as indicated by the *P* value through the Monte Carlo simulation test ($P=0.001$). (I-K) Histograms showing significant increases in the percentage of active neurons out of the total of fura-2-loaded cells (I), the activation rates (Ca^{2+} transients/cell/10^4 seconds) (J) and in number of active cells involved in correlated networks (K), in BDNF-overexpressing hippocampi (black bars) compared to controls (white bars). (L) The average of *P* values obtained by Monte Carlo simulation in co-active networks of transgenic slices (black bars) is much lower than in controls (white bars). $*P<0.01$, $**P<0.001$ Scale bars: 50 μm.

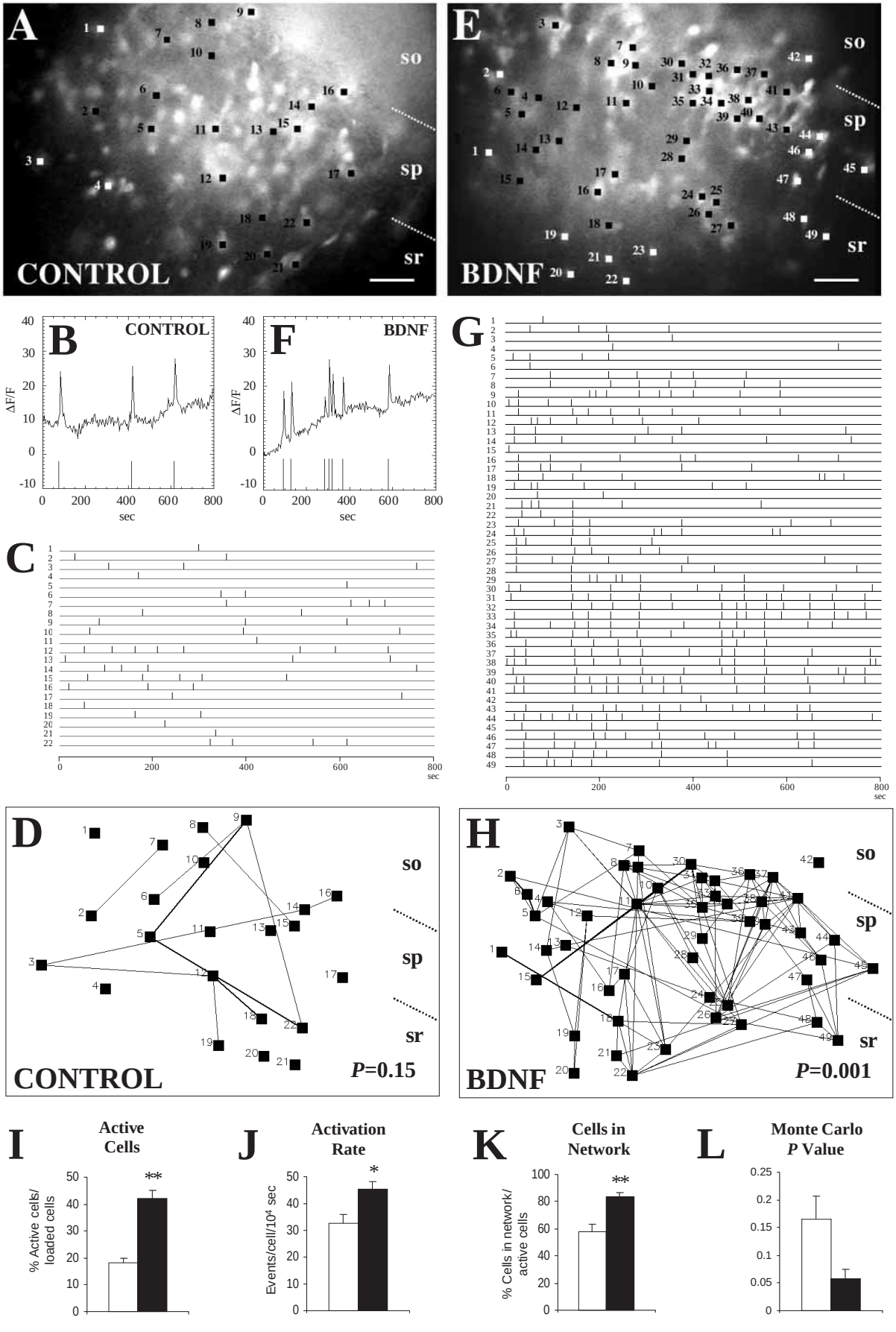
A
CONTROL
so
sp
sr
E
BDNF
so
sp
sr
B
CONTROL
F
BDNF
ΔF/F
sec
C
G
D
CONTROL
P=0.15
H
BDNF
P=0.001
I
Active Cells
% Active cells/ loaded cells
J
Activation Rate
Events/cell/10⁴ sec
K
Cells in Network
% Cells in network/ active cells
L
Monte Carlo P Value

pathways were preserved in these transgenic embryos (Barallobre et al., 2000).

We then investigated the effect of BDNF overexpression on the patterns of spontaneous activity. Recordings of changes of $[Ca^{2+}]_i$ in the CA1 region showed very low levels of spontaneous neuronal activity in wild-type littermates (Fig. 4A-C), with few active neurons (18% of imaged cells) and low frequencies of activation (33 Ca^{2+} transients/cell/10^4 seconds) (Fig. 4I,J). Slices from BDNF-overexpressing mice showed a much greater spontaneous neuronal activity (Fig. 4E-G), with 2.3 times more active neurons (P=0.0001) and 36.3% greater rates of activation (P=0.003) (Fig. 4I,J). We conclude that BDNF overexpression markedly increases spontaneous neuronal activity at embryonic stages in vivo.

To investigate whether BDNF influences the pattern and complexity of spontaneous correlated network activity, we applied the analyses based on contingency tables, χ^2 test and Monte Carlo simulations. Spatiotemporal analysis of wild-type hippocampi revealed a moderate number of cases with significant overall co-activation (Monte Carlo: P<0.05; 55%, 16 out of 29) (Fig. 4L). These correlated networks were simple, and composed of 18±4 neurons, representing about half the active neurons present in the imaged fields (Fig. 4D,K). Similar analyses in BDNF transgenic slices revealed robust synchronous network activity using raster plots (Fig. 4G). Transgenic networks were composed of 38±4 co-activated neurons, 2.1 times more than in controls. Thus, about 83% of the active neurons in BDNF transgenic slices were organized into complex synchronous networks (Fig. 4G,H,K). The proportion of slices showing significant overall network correlation was significantly higher in BDNF transgenic slices (P<0.05; 69%, 29 out of 42 slices) than in control littermates (P<0.05, Bernouilli test). Furthermore, the average P values, obtained by Monte Carlo simulations, were dramatically lower (0.16±0.041 for wild-type versus 0.05±0.016 for transgenic) in *nestin*-BDNF mice (Fig. 4L).

We conclude that prenatal overexpression of BDNF in vivo markedly enhances spontaneous neuronal activity by increasing the number of active neurons and their activation rate. Furthermore, BDNF also triggers the arrangement of such active neurons into highly synchronized correlated networks, which are reminiscent of those observed at P1-P2.

The expression of ionotropic neurotransmitter receptors and their contribution to spontaneous neuronal activity are conserved in BDNF-overexpressing embryos

We next determined whether the expression and distribution of GABA and glutamate receptor subunits were altered in transgenic embryos overexpressing BDNF. Immunoblot analysis of forebrain membranes showed no significant alterations in the levels of the α1 (Fig. 5A) or α2 (data not shown) subunits of the $GABA_A$ receptors. Similarly, no changes were observed in the expression of the NR1, NR2A, GluR1 or GluR2/3 subunits (Fig. 5A). To assess whether the expression and distribution of these subunits might have been altered, we performed immunocytochemical studies. The α2 $GABA_A$, NR1, GluR1 and GluR2/3 subunits were highly expressed in control hippocampi at E18 (Fig. 5B-D). Moderate expression was found for the NR2A subunit and no signals were detected for the α1 $GABA_A$ subunit (see Fritschy et al., 1994). Immunolabeling was mainly present in the plexiform layers, where the dendrites of the principal neurons are located (Fig. 5B-D). No alterations were observed in either the expression levels or the distribution of the α2 $GABA_A$, NR1, GluR1 and GluR2/3 subunits (Fig. 5E-G).

Next, we analyzed the effect of neurotransmitter receptor blockade on the patterns of network activity (Fig. 5H-L). Administration of the $GABA_A$ receptor antagonist BMI (30 μM) to wild-type E18 hippocampal slices dramatically reduced (55%) the number of spontaneously active cells (Fig. 5J). However, the neurons that remained active showed only a slight reduction (less than 13%) in their activation rates (Fig. 5K). The effect of BMI on the complexity of co-active networks was also pronounced (Fig. 5H,I), with a reduction of 68% in the number of neurons belonging to correlated networks (Fig. 5L). Similar, though less marked, reductions in the percentages of active neurons and neurons present in correlated networks were observed after NMDA blockade with APV (50 μM). Only minor changes could be observed in slices treated with the non-NMDA antagonist CNQX (20 μM) (Fig. 5J-L). We conclude that spontaneous network activity at embryonic stages is controlled by $GABA_A$ ionotropic receptors and, to a lesser extent, by NMDA glutamate receptors, which is consistent with analyses at early postnatal stages (Ben-Ari et al., 1997; Garaschuk et al., 1998; Ben-Ari, 2001). A similar analysis on *nestin*-BDNF transgenic embryos showed comparable reductions in the percentages of both active neurons and neurons in correlated networks, after treatment with BMI and APV, and no major alterations after incubation with CNQX (Fig. 5H-L). However, the blockade of spontaneous activity by BMI in BDNF transgenic embryos was less efficient than in control slices (Fig. 5J,L).

These results show that the major GABA and glutamate receptor subunits are present at E18 in the hippocampus, and that these receptors are required for the generation of networks of synchronous spontaneous activity. Our findings also indicate that BDNF overexpression at embryonic stages does not substantially alter either the expression of the receptor subunits or their physiological contribution to the generation of network activity.

Overexpression of BDNF at embryonic stages increases GABAergic and non-GABAergic synaptogenesis and increases $GAD_{65/67}$ expression

Since BDNF could be promoting synaptogenesis at early stages of development, we analyzed the levels of expression of several presynaptic markers (Fig. 6A-C). Immunoblotting of forebrain membranes and immunostaining of hippocampal sections showed no changes in the expression levels or distribution of the synaptic vesicle markers synaptophysin and synapsin I, or the t-SNARE syntaxin 1 (Fig. 6A-C). However, these proteins may not be unequivocal presynaptic markers since they are also distributed along axonal tracts at early developmental stages (Soriano et al., 1994). We therefore used electron microscopy (EM) to count the synaptic contacts. Developing synapses at E18 were immature in appearance, displaying few synaptic vesicles and short synaptic specializations (Fig. 6D,E) (see also Blue and Parnavelas, 1983; Vaughn, 1989; Fiala et al., 1998). Synaptic contacts seemed to be more frequent in transgenic than in control

hippocampi, regardless of the plexiform layer analyzed. Thus, we counted the number of synapses in 3 wild-type and 3 transgenic embryos. BDNF transgenic embryos had 63% more synapses (P=0.0017) than control littermates in the stratum radiatum (Fig. 6F). We conclude that BDNF overexpression produces a marked increase in the total number of synaptic contacts in the embryonic hippocampus.

We also observed that transgenic axon terminals displayed 59.5% fewer synaptic vesicles than terminals from control mice (Fig. 6D,E,G). However, the number of synaptic vesicles clustered near the active zone (see Materials and Methods) was higher in BDNF-overexpressing embryos (P<0.0001) (Fig. 6H). These results suggest alterations in the exocytotic cycle of synaptic vesicles in BDNF-overexpressing embryos.

Postsynaptic elements were usually large in size and displayed microtubules, thus most likely corresponding to dendrites (Fig. 6D,E). Visual inspection of the electromicrographs suggested that postsynaptic dendrites were larger in transgenic hippocampi (Fig. 6D,E). We thus measured the surface area of postsynaptic elements in wild-type and

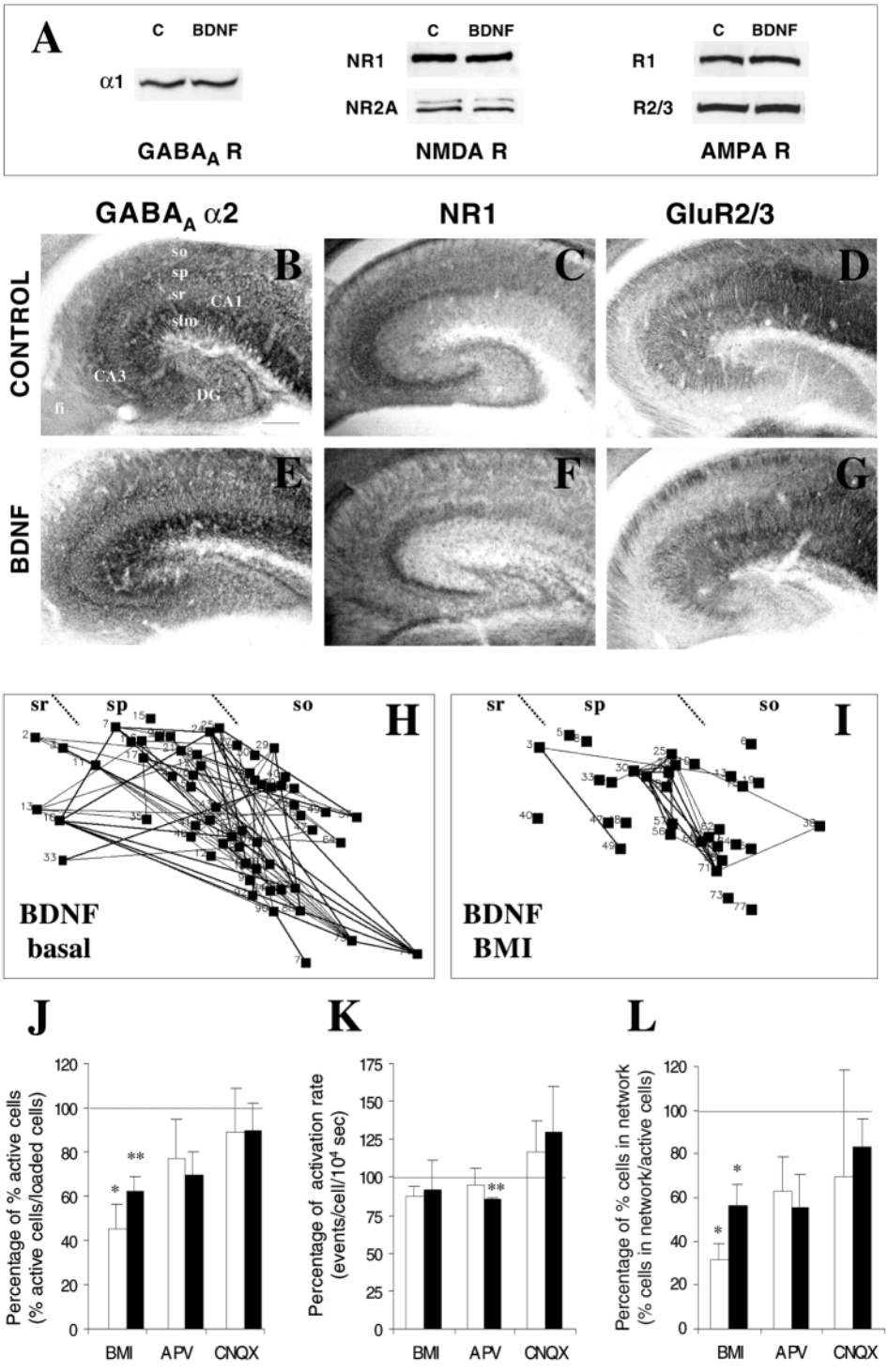

Fig. 5. Expression and contribution of neurotransmitter receptors in the BDNF-overexpressing hippocampus. (A) Western blot analysis of the GABA$_A$ receptor α1 subunit and the glutamate receptor NR1, NR2A, GluR1 and GluR2/3 subunits in membrane fractions isolated from wild-type (C) and transgenic (BDNF) forebrains at E18. There are no differences between groups. (B-G) Immunostaining for the GABA$_A$ α2 (B,E), NR1 (C,F) and GluR2/3 subunits (D,G) in control (B-D) and BDNF-overexpressing (E-G) E18 hippocampal sections. These subunits are distributed in a similar way throughout the hippocampal formation of control and transgenic embryos. In addition, no major changes in the density of immunostaining were observed. (H,I) Representative paired correlation maps showing spontaneous correlated network activity in the CA1 region of a transgenic hippocampal slice before (H) and after (I) blocking GABA$_A$ receptors by administration of 30 μM BMI. Note that GABA$_A$ receptor blockade decreases correlated network complexity. (J-L) Histograms showing the percentage of active neurons (J), the activation rate (K) and the number of active cells in spontaneous correlated networks (L) in the E18 CA1 region after incubations with the GABA$_A$, NMDA and AMPA/kainate antagonists BMI, APV and CNQX, respectively. Data are stardardized to baseline values. White bars represent wild-type and black bars, transgenic embryos. The number of slices used ranged from 3 to 10 for each experimental condition. BMI incubation blocks spontaneous network activity in both wild-type and transgenic slices. Data are mean ± s.e.m. Significance levels: *P<0.05, **P<0.01, Student t-test. Scale bars, 200 μm. Abbreviations as in Fig. 1.

BDNF-transgenic embryos. As shown in Fig. 6I the area of postsynaptic elements was 1.6 times greater in transgenic embryos (P=0.001). In contrast, there were no differences in the surface area of presynaptic boutons between wild-type and transgenic hippocampi (0.6±0.06 μm^2 versus 0.57±0.05 μm^2, P=0.86) (Fig. 6J).

Because GABA is the main excitatory neurotransmitter at early development stages (Ben-Ari, 2001), we analyzed whether the GABAergic system was altered in BDNF-overexpressing embryos. In wild-type hippocampi, $GAD_{65/67}$ mRNA was expressed at moderate levels in the interneurons in the strata oriens and radiatum (Fig. 7A) (Soriano et al., 1994; Supèr et al., 1998). The hippocampus of BDNF transgenic embryos showed dramatically greater $GAD_{65/67}$ mRNA hybridization, with positive neurons showing very high expression levels (Fig. 7B). Northern blot analysis supported these observations by showing 3-fold greater GAD_{67} mRNA (Fig. 7C). Immunostaining for calbindin (Soriano et al., 1994; Supèr et al., 1998) showed that interneurons had hypertrophied perikarya and dendrites in BDNF transgenic embryos (Fig. 7D,E).

We next examined whether the increase in synaptic contacts in BDNF-overexpressing embryos also applied to GABAergic synapses. In both control and transgenic hippocampi, GABA-positive synaptic contacts were recognized by the presence of gold particles (Fig. 7F-H). The stratum radiatum of BDNF transgenic embryos had 2.9 times more GABA-positive synapses than those of controls (P<0.001) (Fig. 7I). We conclude that BDNF at embryonic stages dramatically increases GABAergic synaptogenesis and $GAD_{65/67}$ mRNA expression, and leads to hypertrophy of the GABAergic interneurons.

Finally, we also quantified the number of GABA-negative synapses. 1.54 times more non-GABAergic synapses (P<0.05) were found in BDNF-transgenic hippocampi (2.4±0.2) than in wild-type embryos (1.55±0.2) (Fig. 7J). We conclude that BDNF overexpression increases both GABAergic and non-GABAergic synaptogenesis.

BDNF overexpression increases expression of the K^+/Cl^- co-transporter KCC2 and alters $GABA_A$-evoked responses

During early stages of development, activation of $GABA_A$ receptors induces Cl^- efflux, which results in high depolarization and triggers a rise in $[Ca^{2+}]_i$ (Cherubini et al.,

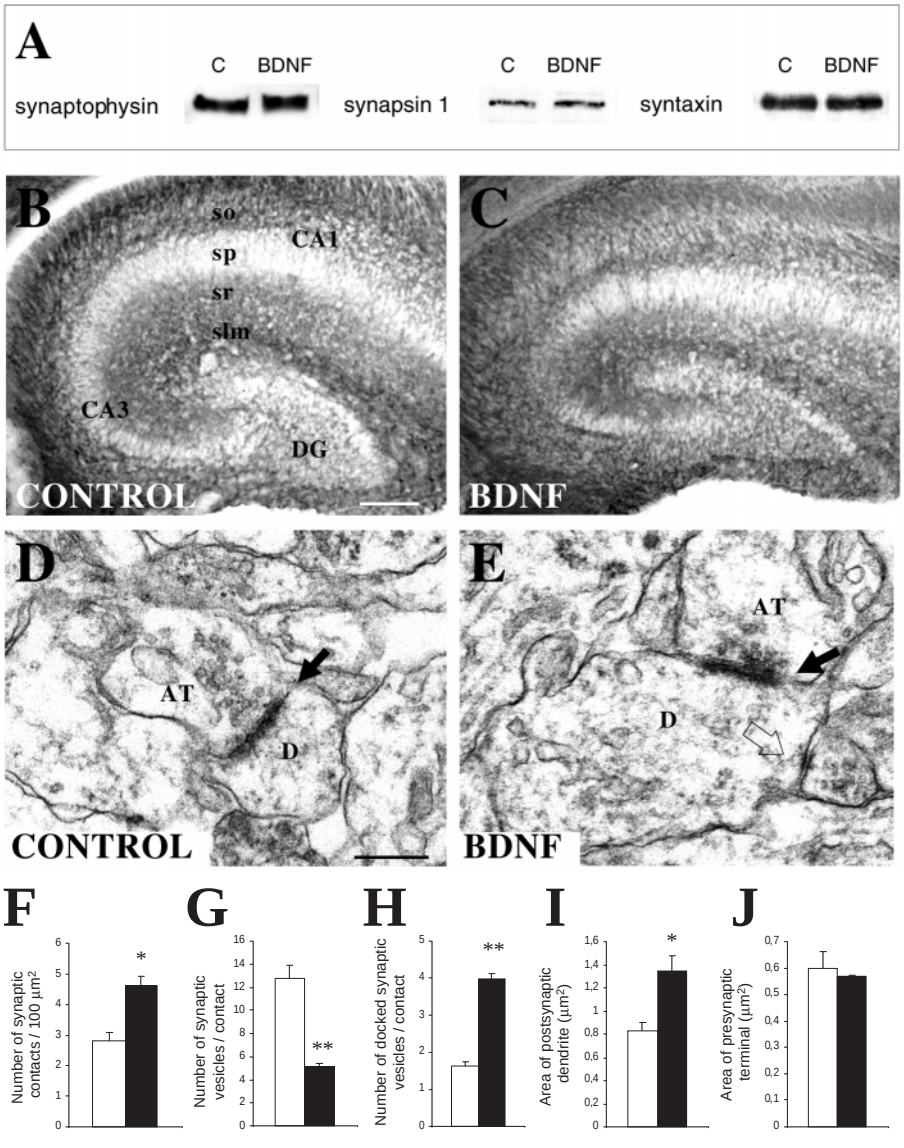

Fig. 6. Transgenic BDNF-overexpressing embryos show increased hippocampal synaptogenesis. (A) Immunoblot analysis of the synaptic vesicle proteins synaptophysin and synapsin I, and of the t-SNARE syntaxin1 in forebrain membrane fractions from control (C) and transgenic (BDNF) E18 embryos reveals no major differences between groups. (B,C) Photomicrographs illustrating similar patterns of immunolabeling were observed for synaptophysin in hippocampal sections from wild-type (B) and BDNF-overexpressing (C) E18 embryos. (D,E) Electron micrographs illustrating synaptic contacts (black arrows) in the stratum radiatum of control (D) and transgenic (E) E18 embryos. Note the distinct patterns of distribution of synaptic vesicles in the axon terminal and the increased area of postsynaptic dendrite of transgenic synapses. Open arrow in E points to a putative contact. (F-J) Quantitative analysis illustrating structural alterations in synaptic profiles of E18 transgenic hippocampi. BDNF-overexpressing embryos show a significant increase in the number of synaptic contacts per area (F) and in the number of docked synaptic vesicles per contact (H), whereas the total number of synaptic vesicles per contact is significantly decreased in these embryos compared to wild-type embryos (G). The area of postsynaptic dendrites was significantly increased in transgenic embryos (I) whereas no differences were found for axon terminal area between both groups of animals (J). Values are mean ± s.e.m. White bars, wild type; black bars, transgenic embryos. *P<0.01; **P<0.0001. Scale bars, 400 μm (B,C); 0.5 μm (D,E). AT, axon terminal; D, dendrite; so, sp, sr, slm, CA1, CA3 and DG as in Fig. 1.

1991; Ben-Ari, 2001). As development progresses, $[Cl^-]_i$ decreases and the response of $GABA_A$ receptors switch from excitation to inhibition, in a process which depends on the regulated expression of the KCC2 K^+/Cl^- co-transporter (Rivera et al., 1999). Given that GABA triggers the expression of KCC2 (Ganguly et al., 2001) and the enhancement of the GABAergic system observed in BDNF-overexpressing embryos, we examined whether BDNF had a function in the regulation of KCC2 expression. RT-PCR analysis showed very low KCC2 mRNA expression in the forebrain of E18 control embryos. In contrast, high expression (4.3-fold greater) was detected in the forebrains of BDNF-overexpressing embryos (Fig. 8A). To determine whether KCC2 mRNA was expressed in the hippocampus, we performed in situ hybridization. Whereas control hippocampi were almost devoid of KCC2 mRNA, strong hybridization signals were detected in BDNF transgenic hippocampi in both the pyramidal and granule cell layers (Fig. 8B,C). We conclude that BDNF dramatically increases KCC2 expression.

We explored whether the precocious expression of KCC2 altered the response of $GABA_A$ receptor activation, by analysing by $[Ca^{2+}]_i$ imaging the response of hippocampal neurons to the $GABA_A$ receptor agonist muscimol (Fig. 8D,E). No significant differences in the number of neurons responding to the agonist by $[Ca^{2+}]_i$ increases were noted (Fig. 8F). However, the amplitude of muscimol-evoked responses was 43% lower in BDNF-overexpressing hippocampi than in wild-type littermates ($P<0.0001$) (Fig. 8D-F), indicating that the fast excitatory action of GABA through $GABA_A$ receptors is attenuated in these mutants. Taken together, these findings indicate that the expression of the KCC2 co-transporter in

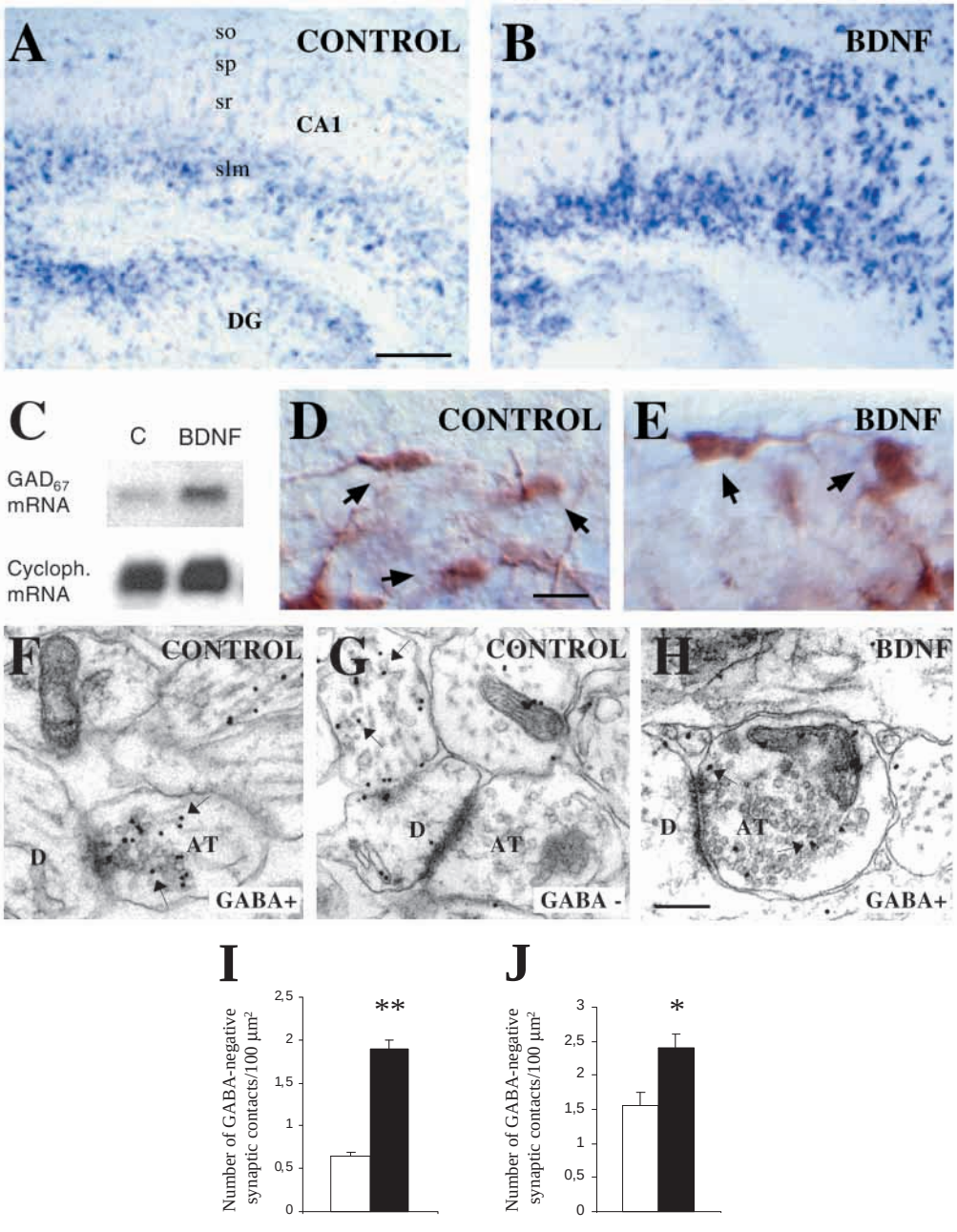

Fig. 7. $GAD_{65/67}$ expression and GABAergic synaptic contacts are greater in the E18 BDNF-overexpressing hippocampus. (A,B) Non-radioactive in situ hybridization showing the expression patterns of $GAD_{65/67}$ in the embryonic wild-type (A) and transgenic (B) hippocampus at E18. Note the increased hybridization signals in the transgenic hippocampus. (C) Northern blot analysis of E18 forebrain showing a 3-fold increase in GAD_{67} mRNA expression in transgenic embryos (BDNF) compared to control embryos (C). Cyclophylin mRNA levels were used as an internal standard. (D,E) High magnification photomicrographs illustrating calbindin-immunopositive interneurons (arrows) in the stratum oriens of control (D) and transgenic (E) E18 hippocampi. Note the larger calbindin-positive neurons in the BDNF transgenic embryos compared to controls (arrows). (F-H) Electron microphotographs showing GABA immunogold labeling (arrows) in the stratum radiatum of E18 wild-type (F,G) and transgenic (H) hippocampus exhibiting GABA-positive (F,H) and GABA-negative (G) axon terminals (AT) with dendrites (D). (I,J) Histograms representing the greater number of GABA-positive axon terminals (I) and GABA-negative axon terminals (J) in BDNF-overexpressing hippocampus (black bar) than in wild-type hippocampus (white bar). $*P<0.05$; $**P<0.001$. Scale bars: 300 µm (A,B); 20 µm (D,E); 0.4 µm (F,G). Abbreviations as in Fig. 1.

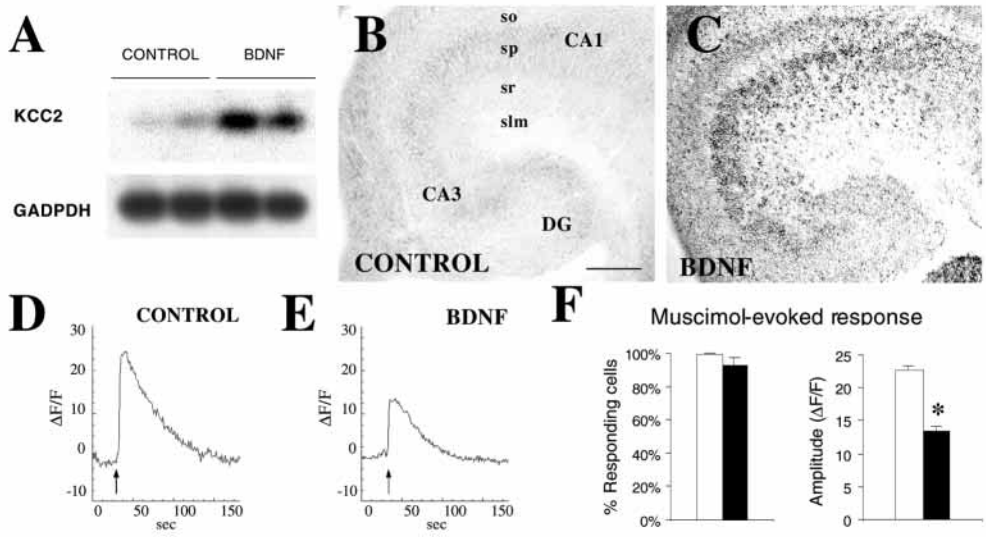

Fig. 8. BDNF-overexpression alters KCC2 mRNA expression and $GABA_A$ receptor-evoked responses in E18 transgenic embryos. (A) Semiquantitative RT-PCR analysis showing the expression levels of KCC2 mRNA in two wild-type (control) and two transgenic (BDNF) forebrains. Note the marked increase in KCC2 mRNA levels in BDNF-overexpressing embryos compared to controls. GAPDH RT-PCR analysis was used as reference. (B,C) Non-radioactive in situ hybridizations illustrating neuronal somata expressing consistent levels of KCC2 mRNA through the hippocampus of transgenic BDNF-overexpressing embryos (C), whereas KCC2 mRNA expression levels in the control hippocampus are close to background (B). (D,E) Plot of ΔF/F over time illustrating representative examples of $GABA_A$-evoked responses in wild-type (control) and transgenic (BDNF) neurons from E18 hippocampal slices. Administration of 10 μM muscimol (arrows) caused a $[Ca^{2+}]_i$ increase in both control and transgenic neurons, although the response was impaired in BDNF-overexpressing embryos (E). (F) Histograms representing the percentage of neurons responding to muscimol by $[Ca^{2+}]_i$ increase and the ΔF/F amplitude in control (white bars) and BDNF-overexpressing hippocampi (black bars). Values are mean ± s.e.m. Scale bar: 200μm. *P<0.0001. Abbreviations as in Fig. 1.

BDNF transgenic embryos reduces $GABA_A$-evoked $[Ca^{2+}]_i$ increases by decreasing $[Cl^-]_i$.

DISCUSSION

The present study shows a non-oscillatory form of spontaneous correlated network activity, which is present in the embryonic hippocampus from E16 onwards. We show that the emergence of robust correlated activity after birth is linked to a non-linear increase in the number of active neurons recruited (see Fig. 2L), which supports the view that spontaneous networks depend on a threshold of functional connectivity and level of released neurotransmitters (O'Donovan, 1999; Ben-Ari, 2001). Our observations show that $GABA_A$ and NMDA glutamate receptors are needed to generate spontaneous activity and correlated networks in the embryonic hippocampus, which suggest that the same signaling systems drive spontaneous activity at prenatal and postnatal ages (Ben-Ari et al., 1997; Garaschuk et al., 1998; Ben-Ari, 2001). We conclude that the synaptic and neurotransmitter systems triggering spontaneous neuronal activity and network correlations emerge long before birth, although robust networks recruiting almost the entire population of neurons only appear after birth.

Here we used a gain-of-function mouse model to investigate possible functions of BDNF at early stages. Whereas expression of BDNF at E18 in wild-type forebrains is very low, *nestin*-BDNF transgenic embryos show a marked increase in BDNF expression, reaching levels similar to those detected at postnatal stages in control mice (Ringstedt et al., 1998). Because endogenous TrkB receptors are expressed at normal levels in *nestin*-BDNF transgenic embryos (C. F. Ibañez, personal communication), we analyzed the effect of early physiological activation of endogenous TrkB receptors on the patterns of neuronal activity. We show that BDNF overexpression dramatically increases the number of neurons exhibiting spontaneous $[Ca^{2+}]_i$ transients in vivo, and that BDNF may also increases correlated spontaneous network activity. Because most hippocampal neurons are generated at E13-E16 (Soriano et al., 1989), we examined 2- to 5-day-old postmitotic neurons (E18) and show that they respond to BDNF by acquiring activity profiles which are typical of P1-P2 postnatal neurons. We conclude that BDNF may be a potent regulator of spontaneous neuronal network activity at embryonic stages, and that young postmitotic neurons are very sensitive to BDNF dosage.

Both the developmental profile and the plasticity of early spontaneous network activity in the CNS suggest that homeostatic factors modulate the properties of this activity (Feller, 1999; O'Donovan, 1999). However, the identity of such factors remains unknown. The present results, indicating that neuronal network activity is controlled by BDNF, along with the findings that BDNF and TrkB are themselves regulated by neural activity and neurotransmitter-dependent $[Ca^{2+}]_i$ changes (Ernfors et al., 1991; Berninger et al., 1995; Kohara et al., 2001), support a homeostatic role for BDNF in the regulation of early spontaneous activity and in their organization into correlated functional networks.

Axon terminals in BDNF transgenic embryos have higher numbers of synaptic vesicles docked at the active zones, and a lower density of synaptic vesicles, in agreement with reports proposing a role for BDNF in the modulation of the docking

vesicle step (Pozo-Miller et al., 1999). This suggests that neurotransmitter release may be enhanced in BDNF transgenic embryos (Südhof, 2000). The role of BDNF in CNS synaptogenesis has previously been investigated at postnatal ages or at the equivalent stages in vitro (Martinez et al., 1998; Vicario-Abejón et al., 1998; Pozo-Miller et al., 1999), which raises the possibility that the effects observed may be a consequence of either altered formation or rearrangement of synaptic contacts. Our data showing increased numbers of synaptic contacts at the onset of hippocampal synaptogenesis strongly suggest that early synapse formation in vivo is indeed regulated by BDNF.

We show that overexpression of BDNF regulates the development of the GABAergic system, as evidenced by somata hypertrophy, enhanced $GAD_{65/67}$ expression and increased synaptogenesis, suggesting that BDNF may act on cortical GABAergic synaptogenesis in vivo at earlier stages than previously reported (Marty et al., 1997; Vicario-Abejón et al., 1998; Huang et al., 1999). Because GABA is the principal excitatory transmitter in the neonatal brain (Ben-Ari, 2001), the increased maturation of the GABAergic system is likely to underlie the increased levels of synchronous network activity in BDNF-overexpressing hippocampi. Since GABAergic neurons develop before pyramidal neurons and play a role in the maturation of glutamatergic transmission (Soriano et al., 1989; Ben-Ari et al., 1997; Ben-Ari, 2001), GABAergic neurons may be the earliest target of BDNF, controlling the development of the entire hippocampal network.

Conversion of GABAergic transmission from depolarizing to hyperpolarizing depends on the expression of KCC2 and the Cl^- electrochemical potential (Ben-Ari et al., 1997; Rivera et al., 1999; Hüber et al., 2001). We found that BDNF overexpression increases the expression of KCC2 and reduces the amplitude of Ca^{2+} transients evoked by activation of $GABA_A$ receptors. A steady increase in KCC2 expression, concomitant with decreased amplitude of $GABA_A$-evoked Ca^{2+} responses, occurs from embryonic to postnatal stages (Garaschuck et al., 1998; Rivera et al., 1999; Ganguly et al., 2001; Hüber et al., 2001; Gulyás et al., 2001; Owens et al., 1996). As the KCC2 expression levels and $GABA_A$ responses in E18 BDNF transgenic neurons are similar to those found in early postnatal hippocampi (Garaschuk et al., 1998; Rivera et al., 1999; Gulyas et al., 2001), we suggest that BDNF controls the developmental switch of GABAergic transmission.

KCC2 expression is associated with reduced $GABA_A$-evoked $[Ca^{2+}]_i$ responses (Garaschuck et al., 1998; Rivera et al., 1999; Ganguly et al., 2001; Hüber et al., 2001; Gulyás et al., 2001; Owens et al., 1996). However, both the $GABA_A$ blockade by BMI in transgenic slices and the muscimol-induced $[Ca^{2+}]_i$ increases in virtually all transgenic hippocampal neurons indicate that GABA is still excitatory, despite the expression of KCC2. The situation is similar to that at early postnatal stages in the hippocampus (P1-P4), when KCC2 expression levels are not high enough to convert $GABA_A$ responses into inhibitory actions (Rivera et al., 1999), and robust spontaneous activity is still essentially driven by $GABA_A$ depolarizing responses (Ben-Ari, 2001; Garaschuk et al., 1998). Consistent with this, the present physiological and pharmacological analyses show that the contribution of $GABA_A$-evoked excitation in acute slices (Fig. 5H-L) and of muscimol-induced Ca^{2+} responses (Fig. 8D-F) are decreased in BDNF-transgenic embryos.

In summary, the present study indicates that BDNF regulates the emergence and complexity of spontaneous co-active networks in vivo, which demonstrates a new level of regulation of neuronal circuits by neurotrophins. We also show that the mechanisms controlling spontaneous activity include the convergent actions of increased synaptogenesis and GABAergic development, as well as the accelerated conversion of GABAergic responses through the regulation of KCC2 expression. Because $[Ca^{2+}]_i$ oscillations regulate numerous developmental processes, which are in turn amplified among vast numbers of neurons by synchronous patterns of activity (Komuro and Rakic, 1998; Spitzer et al., 2000; Feller, 1999; Buonanno and Fields, 1999), the control of network activity by BDNF is likely to regulate patterned gene expression and synaptic circuits. Since spontaneous network activity reflects the pattern of intrinsic circuits (Yuste et al., 1995; Feller, 1999; Ben-Ari, 2001; Mao et al., 2001), BDNF may control the properties and complexity of the basic circuits operating in neuronal processing. The data also suggest that the effects of BDNF on activity-dependent plasticity (Bonhoeffer, 1996; McAllister et al., 1999; Schuman, 1999; Schinder and Poo, 2000) could be mediated in part by the regulation of the complexity of intrinsic circuits and networking properties.

We are grateful to Drs J. M. Fritschy (Zurich), A. Tobin (Los Angeles), M. Watanabe (Sapporo) and F. G. Rathjen (Berlin) for the generous gift of antibodies against GABA and NMDA receptor subunits and L1, and of GAD probes. We also thank Drs J. A. Del Rio, T. Ringstedt, J. V. Sanchez-Andres, J. Blasi, M. Solé and M. J. Barallobre for providing some *nestin*-BDNF embryos and for help in some experiments, and Robin Rycroft for editorial assistance. This study was supported by grants from CICYT (SAF98-106, FEDER-2FD97-1760-C03-01, SAF01-3098, SAF01-134 and BFI2001-3186), FIS (99/0622 and 01/1684), the EU (Biotech Program II) and Caixa Foundation to E. S., F. A., F. J. M.-G. and S. A., the NEI (EY11787 and EY13237) and NINDS (NS40726) to R. Y., and from the Swedish Medical Research Council (K99-33X-10908-06C) to C. F. I. M. A. C. is recipient of a fellowship from MECD.

REFERENCES

Aguiló, A., Schwartz, T. H., Kumar, V. S., Peterlin, Z. A., Tsiola, A., Soriano, E. and Yuste, R. (1999). Involvement of Cajal-Retzius neurons in spontaneous correlated activity of embryonic and postnatal layer 1 from wild-type and reeler mice. *J. Neurosci.* **19**, 10856-10868.

Alsina, B., Vu, T. and Cohen-Cory, S. (2001). Visualizing synapse formation in arborizing optic axons in vivo: dynamics and modulation by BDNF. *Nat. Neurosci.* **4**, 1093-1101.

Barallobre, M. J., del Rio, J. A., Alcántara, S., Borrell, V., Aguado, F., Ruiz, M., Carmona, M. A., Martin, M., Fabre, M. Yuste, R. et al. (2000). Aberrant development of hippocampal circuits and altered neuronal activity in netrin 1-deficient mice. *Development* **127**, 4797-4810.

Ben-Ari, Y., Cherubini, E., Corradetti, B. and Gaiarsa, J. L. (1997). $GABA_A$, NMDA and AMPA receptors: a developmentally regulated 'ménage à trois'. *Trends Neurosci.* **20**, 523-529.

Ben-Ari, Y. (2001). Developing networks play a similar melody. *Trends Neurosci.* **24**, 353-360.

Berninger, B., Marty, S., Zafra, F., Berzaghi, M. P., Thoenen, H. and Lindholm, D. (1995). GABAergic stimulation switches from enhancing to repressing BDNF expression in rat hippocampal neurons during maturation in vitro. *Development* **121**, 2327-2335.

Blue, M. E. and Parnavelas, J. G. (1983). The formation and maturation of synapses in the visual cortex of the rat. I. Qualitative analysis. *J. Neurocytol.* **12**, 599-616.

Bonhoeffer, T. (1996). Neurotrophins and activity-dependent development of the neocortex. *Curr. Opin. Neurobiol.* **6**, 119-126.

Buonanno, A. and Fields, R. D. (1999). Gene regulation by patterned electrical activity during neural and skeletal muscle development. *Curr. Opin. Neurobiol*. **9**, 110-120.

Cherubini, E., Gaiarsa, J. L. and Ben-Ari, Y. (1991). GABA: an excitatory transmitter in early postnatal life. *Trends Neurosci.* **14**, 515-519.

Crespo, C., Blasco-Ibáñez, J. M., Briñón, J. G., Alonso, J. R., Domínguez, M. I. and Martínez-Guijarro, F. J. (2000). Subcellular localization of m2 muscarinic receptors in GABAergic interneurons of the olfactory bulb. *Eur. J. Neurosci.* **12**, 3963-3974.

Diabira, D., Hennou, S., Chevassus-au-Louis, N., Ben-Ari, Y. and Gozlan, H. (1999). Late embryonic expression of AMPA receptor function in the CA1 region of the intact hippocampus in vitro. *Eur. J. Neurosci.* **11**, 4015-4023.

Erlander, M. G., Tillakaratne, N. J., Feldblum, S., Patel, N. and Tobin, A. J. (1991). Two genes encode distinct glutamate decarboxylases. *Neuron* **7**, 91-100.

Ernfors, P., Begzon, J., Kokaia, Z., Persson, H. and Lindvall, O. (1991). Increased levels of messenger RNAs for neurotrophic factors in the brain during kindling epileptogenesis. *Neuron* **7**, 165-176.

Feller, M. B. (1999). Spontaneous correlated activity in developing neural circuits. *Neuron* **22**, 653-656.

Fiala, J. C., Feinberg, M., Popov, V. and Harris, M. (1998). Synaptogenesis via dendritic filopodia in developing hippocampal area CA1. *J. Neurosci*. **18**, 8900-8911.

Fritschy, J. M., Paysan, J., Enna, A. and Mohler, H. (1994). Switch in the expression of rat $GABA_A$-receptor subtypes during postnatal development: an immunohistochemical study. *J. Neurosci.* **14**, 5302-5324.

Ganguly, K., Schinder, A. F., Wong, S. T. and Poo, M. M. (2001). GABA itself promotes the developmental switch of neuronal GABAergic responses from excitation to inhibition. *Cell* **105**, 521-532.

Garaschuk, O., Hanse, E. and Konnerth, A. (1998). Developmental profile and synaptic origin of early network oscillations in the CA1 region of rat neonatal hippocampus. *J. Physiol.* **507**, 219-236.

Gulyás, A. I., Sík, A., Payne, J. A., Kaila, K. and Freund, T. F. (2001). The KCl cotransporter, KCC2, is highly expressed in the vicinity of excitatory synapses in rat hippocampus. *Eur. J. Neurosci.* **13**, 2205-2217.

Huang, Z. J., Kirkwood, A., Pizzorusso, T., Porciatti, V., Morales, B., Bear, M. F., Maffei, L. and Tonegawa, S. (1999). BDNF regulates the maturation of inhibition and the critical period of plasticity in mouse visual cortex. *Cell* **98**, 739-755.

Huang, E. L. and Reichardt, L. F. (2001). Neurotrophins: roles in neuronal development and function. *Annu. Rev. Neurosci.* **24**, 677-736.

Hüber, C. A., Stein, V., Hermans-Borgmeyer, I., Meyer, T., Ballanyi, K. and Jentsch, T. (2001). Disruption of KCC2 reveals an essential role of K-Cl cotransport already in early synaptic inhibition. *Neuron* **30**, 515-524.

Katz, L. C. and Shatz, C. J. (1996). Synaptic activity and the construction of cortical circuits. *Science* **274**, 1133-1138.

Knüsel, B., Rabin, S. J., Hefti, F. and Kaplan, D. R. (1994). Regulated neurotrophin receptor responsiveness during neuronal migration and early differentiation. *J. Neurosci.* **14**, 1542-1554.

Kohara, K., Kitamura, A., Morishima, M. and Tsumoto, T. (2001). Activity-dependent transfer of brain-derived neurotrophic factor to postsynaptic neurons. *Science* **291**, 2419-2423.

Komuro, H. and Rakic, O. (1998). Orchestration of neuronal migration by activity of ion channels, neurotransmitter receptors, and intracellular Ca^{2+} fluctuations. *J. Neurobiol.* **37**, 110-130.

Mao, B.-Q., Hamzei-Sichani, F., Aronov, D., Froemke, R. C. and Yuste, R. (2001). Dynamics of spontaneous activity in neocortical slices. *Neuron* **32**, 883-898.

Martínez, A., Alcántara, S., Borrell, V., del Río, J. A., Blasi, J., Otal, R., Campos, N., Boronat, A., Barbacid, M., Silos-Santiago, I. et al. (1998). TrkB and TrkC signaling are required for maturation and synaptogenesis of hippocampal connections. *J. Neurosci.* **18**, 7336-7350.

Marty, S., Berzaghi, M. P. and Berninger, B. (1997). Neurotrophins and activity-dependent plasticity of cortical interneurons. *Trends Neurosci.* **20**, 198-202.

McAllister, A. K., Katz, L. C. and Lo, D. C. (1999). Neurotrophins and synaptic plasticity. *Annu. Rev. Neurosci.* **22**, 295-318.

O'Donovan, M. J. (1999). The origin of spontaneous activity in developing networks of the vertebrate nervous system. *Curr. Opin. Neurobiol.* **9**, 94-104.

Owens, D. F., Boyce, L. H., Davis, M. B. E. and Kriegstein, A. R. (1996). Excitatory GABA responses in embryonic and neonatal cortical slices demonstrated by gramicidin perforated-patch recordings and calcium imaging. *J. Neurosci.* **16**, 6414-6423.

Penn, A. A., Riquelme, P. A., Feller, M. B. and Shatz, C. J. (1998). Competition in retinogeniculate pattering driven by spontaneous activity. *Science* **279**, 2108-2112.

Pozzo-Miller, L. D., Gottschalk, W., Zhang, L., McDermott, K., Du, J., Gopalakrishnan, R., Oho, C., Sheng, Z. H., Lu, B. (1999). Impairments in high-frequency transmission, synaptic vesicle docking, and synaptic protein distribution in the hippocampus of BDNF knockout mice. *J. Neurosci.* **19**, 4972-4983.

Ringstedt, T., Linnarsson, S., Wagner, J., Lendahl, U., Kokaia, Z., Arenas, E., Ernfors, P. and Ibañez, C. F. (1998). BDNF regulates reelin expression and Cajal-Retzius cell development in the cerebral cortex. *Neuron* **21**, 305-315.

Rivera, C., Voipio, J., Payne, J. A., Ruusuvuori, E., Lahtinen, H., Lamsa, K., Pirvola, U., Saarma, M. and Kaila, K. (1999). The K^+/Cl^- co-transporter KCC2 renders GABA hyperpolarizing during neuronal maturation. *Nature* **397**, 251-255.

Rosahl, T. W., Spillane, D., Missler, M., Herz, J., Selig, D. K., Wolff, J. R., Hammer, R. E., Malenka, R. C. and Südhof, T. C. (1995). Essential function of synapsins I and II in synaptic vesicle regulation. *Nature* **375**, 488-493.

Schinder, A. F. and Poo, M. M. (2000). The neurotrophin hypothesis for synaptic plasticity. *Trends Neurosci.* **23**, 639-645.

Schuman, E. M. (1999). Neurotrophin regulation of synaptic transmission. *Curr. Opin. Neurobiol.* **9**, 105-109.

Schwartz, T., Rabinowtz, D., Unni, V., Kumar, V. S., Smetters, D. K., Tsiola, A. and Yuste, R. (1998). Networks of coactive neurons in developing layer 1. *Neuron* **20**, 541-552.

Soriano, E., Cobas, A. and Fairen, A. (1989). Neurogenesis of glutamic acid decarboxylase immunoreactive cells in the hippocampus of the mouse. I: Regio superior and regio inferior. *J. Comp. Neurol.* **281**, 586-602.

Soriano, E., del Río, J. A., Martínez, A. and Super, H. (1994). Organization of the embryonic and early postnatal murine hippocampus. I. Immunocytochemical characterization of neuronal populations in the subplate and marginal zone. *J. Comp. Neurol.* **342**, 571-595.

Spitzer, N. C., Lautermilch, N. J., Smith, R. D. and Gomez, T. M. (2000). Coding of neuronal differentiation by calcium transients. *BioEssays* **22**, 811-817.

Stellwagen, D. and Shatz, C. J. (2002). An instructive role for retinal waves in the development of retinogeniculate connectivity. *Neuron* **33**, 357-367.

Südhof, T. C. (2000). The synaptic vesicle cycle revisited. *Neuron* **28**, 317-320.

Supèr, H. and Soriano, E. (1994). The organization of the embryonic and early postnatal murine hippocampus. II. Development of entorhinal, commissural, and septal connections studied with the lipophilic tracer DiI. *J. Comp. Neurol.* **344**, 101-120.

Supèr, H., Martinez, A., del Rio, J. A. and Soriano, E. (1998). Involvement of distinct pioneer neurons in the formation of layer-specific connections in the hippocampus. *J. Neurosci*. **15**, 4616-4626.

Vaughn, J. E. (1989). Review: Fine structure of synaptogenesis in the vertebrate central nervous system. *Synapse* **3**, 255-285.

Vicario-Abejón, C., Collin, C., McKay, R. D. and Segal, M. (1998). Neurotrophins induce formation of functional excitatory and inhibitory synapses between cultured hippocampal neurons. *J. Neurosci.* **18**, 7256-7271.

Watanabe, M., Fukaya, M., Sakimura, K., Manabe, T., Mishina, M. and Inoue, Y. (1998). Selective scarcity of NMDA receptor channel subunits in the stratum lucidum (mossy fibre-recipient layer) of the mouse hippocampal CA3 subfield. *Eur. J. Neurosci.* **10**, 478-487.

Yuste, R., Peinado, A. and Katz, L. C. (1992). Neuronal domains in developing neocortex. *Science* **257**, 665-669.

Yuste, R., Nelson, D. A., Rubin, W. W. and Katz, L. C. (1995). Neuronal domains in developing neocortex: mechanisms of coactivation. *Neuron* **14**, 7-17.